Journal Pre-proof

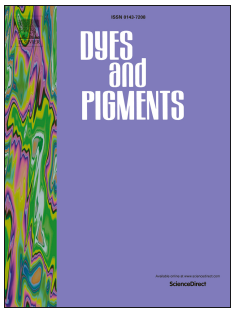

Chalcone-based fluorescent chemosensors as new tools for detecting Cu^{2+} ions

Liliana J. Gomes, Tiago Moreira, Laura Rodríguez, Artur J. Moro

PII: S0143-7208(21)00711-7

DOI: https://doi.org/10.1016/j.dyepig.2021.109845

Reference: DYPI 109845

To appear in: *Dyes and Pigments*

Received Date: 1 July 2021

Revised Date: 29 September 2021

Accepted Date: 30 September 2021

Please cite this article as: Gomes LJ, Moreira T, Rodríguez L, Moro AJ, Chalcone-based fluorescent chemosensors as new tools for detecting Cu^{2+} ions, *Dyes and Pigments* (2021), doi: https://doi.org/10.1016/j.dyepig.2021.109845.

Liliana J. Gomes: Investigation; **Tiago Moreira**: Investigation; **Laura Rodríguez**: Resources, Visualization, Writing - Review & Editing; **Artur J. Moro**: Conceptualization, Investigation, Writing - Original Draft.

GRAPHICAL ABSTRACT

Chalcone-based fluorescent chemosensors as new tools for detecting Cu^{2+} ions

Liliana J. Gomes, [a] Tiago Moreira,[a] Laura Rodríguez,[b,c] Artur J. Moro* [a]

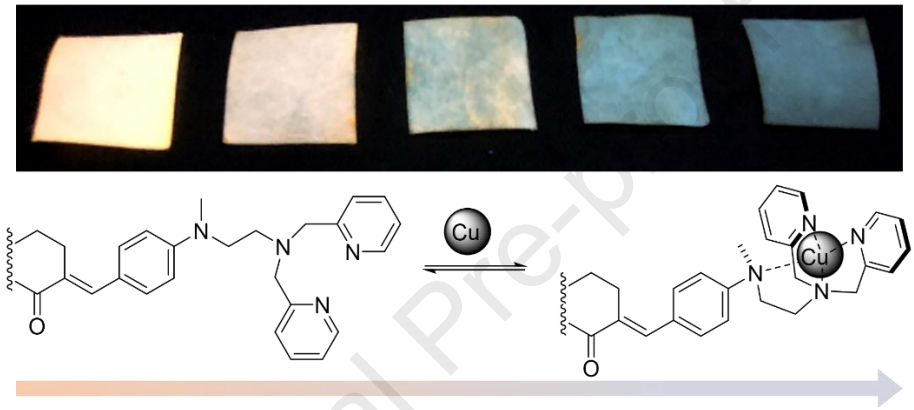

Chalcone-based fluorescent chemosensors as new tools for detecting Cu^{2+} ions

Liliana J. Gomes, [a] Tiago Moreira,[a] Laura Rodríguez,[b,c] Artur J. Moro* [a]

[a]*LAQV-REQUIMTE, Departamento de Química, CQFB, Universidade Nova de Lisboa, Monte de Caparica, Portugal.*

[b]*Departament de Química Inorgànica i Orgànica. Secció de Química Inorgànica. Universitat de Barcelona, Martí i Franquès 1-11, 08028 Barcelona, Spain.*

[c]*Institut de Nanociència i Nanotecnologia (IN^{2}UB). Universitat de Barcelona, 08028 Barcelona, Spain.*

** E-mail:ajm12769@fct.unl.pt*

Abstract

The design and full characterization of new fluorescent chemosensors for Cu^{2+} is herein presented. The structure of the sensors is based on a chalcone backbone as the chromophoric unit, with di-(2-picolyl)amine (DPA) as a receptor moiety. Two systems, bearing one or two chalcone-DPA units, were synthesized and fully characterized.

UV-Vis titrations with several metal ions were performed and both chemosensors exhibited a strong hypsochromic shift in the absorption spectra upon Cu^{2+} addition, indicating a higher selectivity for this metal over other divalent cations. Additionally, fluorescent spectra recorded in the same conditions revealed a stronger quenching effect in the presence of Cu^{2+}, even in the presence of other metal cations, with association constants above 10^6 M^{-1} and detection limits below the micromolar level for both chemosensors. Paper test-strips with one of the chemosensors were prepared to attest its possible application for detecting copper in aqueous samples.

Introduction

Fluorescent chemosensors are molecules capable of binding to a given analyte and produce a quantitatively measurable response in terms of fluorescence change. Over the past century, particularly from the 1980's and beyond, the widespread of fluorescence spectroscopy in various fields of research, especially in Biology and Materials science has led to an exponential growth in the number of developed chemosensors. Given the multitude of possible combinations between fluorophores and binding moieties, a significant number of research groups have been highly successful in creating sensor molecules with outstanding selectivity and tailor-made optical properties.[1]

Coordination chemistry has provided a strong boost creating chemosensor molecules for heavy metal cations, particularly due to their relevance as highly toxic contaminants in Nature.[2] Indeed, the development of different chelating motifs has allowed, not only to detect the presence of relevant heavy metal ions, but also to use the coordinated compound for posterior sensing of anionic and neutral species.[3][4]

A particularly successful example is the di-(2-picolyl)amine (DPA) ligand, which is typically capable of binding divalent cations with some degree of specificity to form stable complexes.[5,6] Coupling the DPA to various fluorophores has led to the development of many fluorescent sensor systems for the detection of Zn^{2+} [7,8] and Cd^{2+} [9][10], typically presenting chelation-enhanced fluorescence (CHEF) in the presence of these metals. However, most of the reported examples also respond strongly to Cu^{2+}, which induces a chelation-quenching effect (CHEQ) due to its paramagnetic character. In fact, successful examples of DPA-based chemosensors can also be found in the literature to be highly selective towards Cu^{2+}, with no response to either Zn^{2+} or Cd^{2+} [11,12] (figure 1a).

In this work, we focused on the design of fluorescent chemosensors bearing DPA units, coupled to chalcone fluorophores [13]. Chalcones are α,β-unsaturated aromatic ketones which are present in many plants, and have been reported to exhibit several therapeutic properties as anti-inflammatory [14,15] and anti-cancer agents [16,17], among others [18–20]. The high chemical versatility of the chalcone core (see figure 1b, highlighted in red) and the ease of their synthetic preparation allows both for fine-tuning their optical properties, as well as the introduction of specific functionalities, which makes them highly attractive targets for the design of new fluorescent chemosensor systems [21]. With this in mind, we synthesized two chalcone derivatives (figure 1b), bearing one or two DPA moieties, and assessed their potential as chemosensors for heavy metal cations.

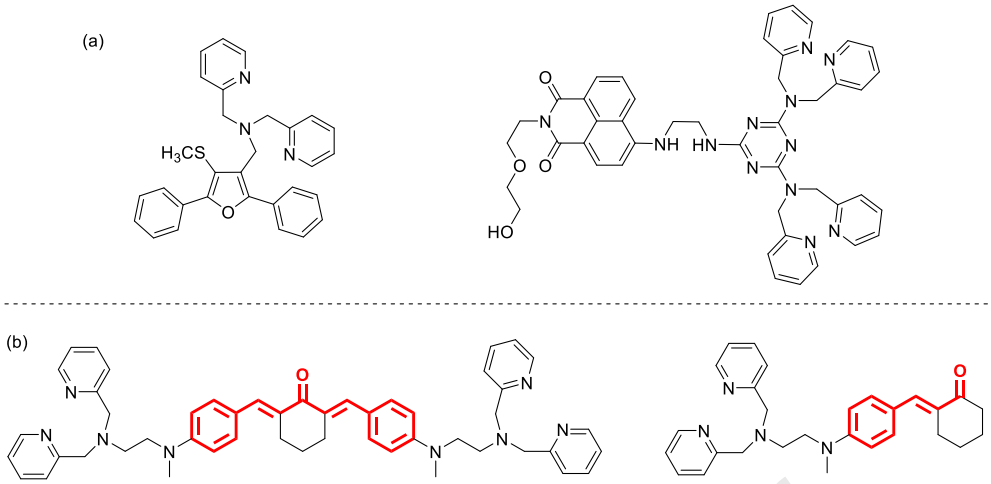

Figure 1. (a) Examples of reported DPA-based chemosensors for Cu^{2+}, from refs. 11 and 12. (b) Chemical structure of DPA-chalcone chemosensors from this work. The chalcone backbone is highlighted in red.

Experimental section

Synthesis

All used chemicals were of analytical grade and used as purchased. Fine chemicals were acquired from Sigma-Aldrich, while solvents were purchased either from Sigma-Aldrich or Carlo Erba.

Synthesis of 2-((4-formylphenyl)(methyl)amino)ethyl 4-methylbenzenesulfonate (**1**)

One equivalent of *N*-Methyl-*N*-(2-hydroxyethyl)-4-aminobenzaldehyde (11.59 g, 0.065 mol) and two equivalents of *p*-toluenesulfonyl chloride (14.88 g, 0.078 mol) were dissolved in dichloromethane (90 mL), and the mixture was cooled to 0ºC in an ice-bath. KOH (4 eqs., 14.59 g, 0.26 mol) was slowly added and the mixture was kept under ice for 3h. Afterwards, dichloromethane (100 mL) and ice-water (200 mL) were added. In a separation funnel, the organic layer was collected, and the aqueous phase was further extracted with dichloromethane (3 × 50 mL). The combined organic layers were washed with water (200 mL), brine (150 mL), and dried with Na_2SO_4. Upon filtration, the solvent was evaporated in a rotatory evaporator, to yield 15.63 g (η = 73%) of pure product as a brown solid. Melting point: 140 – 144 ºC. IR (cm^{-1}): 3052, 3000, 2929, 2809, 1685; 1590; 1343; 1157. ^{1}H NMR (400 MHz, $CDCl_3$) δ 9.74 (s, 1H), 7.68 (d, *J* = 8.7 Hz, 4H), 7.24 (d, *J* = 8.2 Hz, 2H), 6.58 (d, *J* = 8.8 Hz, 2H), 4.20 (t, *J* = 5.7 Hz, 2H), 3.72 (t, *J* = 5.7 Hz, 2H), 3.00 (s, 3H), 2.39 (s, 2H). ^{13}C NMR (100 MHz, $CDCl_3$) δ 190.28, 152.66, 145.15, 132.45, 131.98, 129.87, 127.79, 125.93, 111.10, 66.47, 50.90, 39.30, 21.65. HR-ESI-MS (+) m/z: 334.1101 ($[M + H]^+$, calcd: 334.1108).

Synthesis of 4-((2-(bis(pyridin-2-ylmethyl)amino)ethyl)(methyl)amino)benzaldehyde (**2**)

A solution of **1** (3.42 g, 10.3 mmol), di-(2-picolyl)amine (1.1 eqs., 2.25 g, 11.3 mmol) and potassium carbonate (2 eqs., 2.83 g, 20.6 mmol) in acetonitrile (50 mL) was refluxed for 24h. Afterwards, the reaction mixture was cooled down to room temperature and the solvent was evaporated. The resulting residue was redissolved in dichloromethane (60 mL), and the organic phase was washed with HCl 0.01 M (25 mL), water (2 × 25 mL) and brine (25 mL). The organic phase was then dried with Na_2SO_4, filtered, and the solvent was evaporated. The residue was purified through flash chromatography (DCM/MeOH 15:1, R_f = 0.4) to yield 3.25 g of pure **2** (η = 88%) as a dark brown oil. IR (cm^{-1}): 3052, 2911, 2820, 1665, 1594, 1518, 1380, 1166. ^{1}H NMR (400 MHz, $CDCl_3$) δ 9.62 (s, 1H), 8.48 (d, *J* = 3.7 Hz, 2H), 7.55 (d, *J* = 6.7 Hz, 4H), 7.36 (d, *J* = 7.6 Hz, 2H), 7.12 – 7.03 (m, 2H), 6.49 (d, *J* = 8.6 Hz, 2H), 3.84 (s, 4H), 3.47 (t, *J* = 6.9 Hz, 2H), 2.89 (s, 3H), 2.72 (t, *J* = 6.9 Hz, 2H). ^{13}C NMR (100 MHz, $CDCl_3$) δ 190.17, 158.94, 153.37, 149.19, 136.49, 132.00, 125.02, 123.06, 122.26, 110.81, 60.97, 50.38, 38.82. HR-ESI-MS (+) m/z: 361.2022 ($[M + H]^+$, calcd: 361.2023).

Synthesis of (2E,6E)-2,6-bis(4-((2-(bis(pyridin-2-ylmethyl)amino)ethyl)(methyl)amino)-benzylidene)cyclohexanone (**3**)

To a solution of **2** (3.2 g, 8.9 mmol) and cyclohexanone (0.44 g, 4.4 mmol) in ethanol (40 mL) under an ice bath, NaOH 40% aqueous solution (5 mL) was added dropwise. The solution was

kept under ice for 30 mins, at which point it was allowed to warm up to room temperature and left stirring overnight. The mixture was diluted with water (50 mL), neutralized to pH~7-8 with HCl 6 M and extracted with DCM (1 × 75 mL and 2 × 50 mL). The combined organic extracts were dried with Na_2SO_4, filtered and the volatiles were evaporated in a rotatory evaporator. Flash chromatography with DCM/MeOH 9:1 yielded 2.59 g (η = 74%) of pure **3** as a brown viscous oil. IR (cm^{-1}): 3064, 2973, 2925, 2825, 1658, 1579, 1508, 1437, 1378, 1151, 966. ^{1}H NMR (400 MHz, $CDCl_3$) δ 8.48 (d, *J* = 3.9 Hz, 1H), 7.65 (s, 1H), 7.57 (t, *J* = 7.1 Hz, 1H), 7.43 (d, *J* = 7.5 Hz, 1H), 7.27 (d, *J* = 8.6 Hz, 1H), 7.13 – 7.09 (m, 1H), 6.50 (d, *J* = 8.7 Hz, 1H), 3.89 (s, 4H), 3.49 (s, 2H), 2.87 – 2.74 (m, 7H), 1.74 (m, 1H). ^{13}C NMR (100 MHz, $CDCl_3$) δ 190.04, 158.31, 149.09, 148.99, 137.01, 136.65, 132.51, 132.23, 124.00, 123.32, 122.38, 111.29, 77.34, 77.02, 76.71, 60.64, 50.59, 50.10, 38.57, 28.75, 23.23. HR-ESI-MS (+) m/z: 783.4497 ($[M + H]^+$, calcd: 783.4493).

Synthesis of 2-(4-((2-hydroxyethyl)(methyl)amino)benzylidene)cyclohexan-1-one (**4**)

In a 100 mL round-bottom flask, **2** (1 eq, 4.59 g, 25.64 mmol) was dissolved in ethanol (30 mL). Then, cyclohexanone (10 eq, 26.54 mL, 25.39 mmol) was added to the reaction mixture under vigorous stirring. At last, a solution of NaOH (6 mL, 50% m/m) and water (10 mL) were added. The reaction was monitored by TLC using as eluent DCM: acetone (9:1). After 22h stirring at room temperature, the reaction was complete. The reaction mixture was then neutralized with HCl 6 M, and the crude reaction was dragged with brine and extracted with DCM (3 × 30 mL). Afterwards, the organic extract was dried with Na_2SO_4, filtered and the solvent was removed under reduced pressure and the reaction mixture was dried under vacuum. The 8.3 g of residue were purified through column silica-gel flash chromatography (DCM:acetone (8.5:1.5)) to produce 4.24 g (η = 63.8%) of 2-(4-((2-hydroxyethyl)(methyl) amino)benzylidene) cyclohexan-1-one as yellow/brownish crystals. Melting point: 84 – 85 ºC. IR (cm^{-1}): 3066, 2930, 1660, 1570, 1518, 1423, 1189, 1141. ^{1}H NMR (400 MHz, $CDCl_3$) δ (ppm): 7.51 (s, 1H), 7.38 (d, *J* = 8.6 Hz, 2H), 6.75 (d, *J* = 8.6 Hz, 2H), 3.84 (q, *J* = 5.6 Hz, 2H), 3.55 (t, *J* = 5.7 Hz, 2H), 3.04 (s, 3H), 2.85 (td, *J* = 6.5, 2.1 Hz, 2H), 2.50 (t, *J* = 6.6 Hz, 2H), 1.89 (dd, *J* = 7.5, 4.1 Hz, 2H), 1.77 (t, *J* = 5.8 Hz, 3H). ^{13}C NMR (100 MHz, $CDCl_3$) δ (ppm): δ 201.52, 150.02, 137.15, 132.85, 132.09, 124.09, 111.92, 60.33, 54.77, 40.09, 38.98, 29.23, 23.97, 23.31. HR-ESI-MS (+) m/z: 441.2654 ($[M + H]^+$, calcd: 441.2654). X-ray crystallography data can be found in the Supplementary Material (CCDC deposition number 2090085).

UV-Vis and Fluorescence Measurements

Solutions for UV-Vis absorption and fluorescence measurements were prepared by adding an aliquot of 30 µL of a $3x10^{-4}$ M methanolic solution of chalcones **3** or **4**, to 1470 µL of aqueous buffer, and 1500 µL of methanol p.a., for a final chemosensor concentration of 5 µM. For all metal titrations, 10 mM HEPES buffer at pH 7.0 ± 0.2 was used. pH titrations were performed using buffer. Metal ion titrations were performed by adding a solution containing both metal and chemosensor to a cuvette containing solely the chemosensor, to ensure that the concentration of the latter remained constant. The limit of detection (LOD) of Cu^{2+} was determined according to IUPAC guidelines [22], by measuring five independently prepared samples of chalcone with no metal (blank) and applying the formula: LOD = $3\sigma/b$, where σ represents the standard deviation

of these measurements, and *b* represents the slope over a fixed linear range (0 – 5 μM was selected). Absorption spectra were acquired in a 1 cm quartz cuvette on a Varian Cary 100 Bio UV- spectrophotometer. Emission spectra were obtained in a 1 cm fluorescence quartz cuvette, using a Horiba-Jobin-Yvon SPEX Fluorolog 3.22 spectrofluorometer. Fluorescence quantum yield for **3** and **4** were determined using Acridine Yellow G (ϕ_f = 0.47, in ethanol) and Coumarin 1 (ϕ_f = 0.5, in ethanol) as references, respectively [23,24]. The binding constant for Chalcone-Cu^{2+} was determined by fitting the experimental data to a Henderson-Hasselbalch binding model using the Solver Add-In from Microsoft Excel [25]. Preparation of paper test-strips was performed on medium fibre-free filter paper, from Hollingsworth & Vose Company (Massachusetts, USA). The paper was cut in squares (20 x 20 mm) which were individually immersed for ca. 10 minutes in a methanolic solution of **3** ([**3**] = 0.284 mM). Afterwards, the paper strips were air-dried (ca. 15 minutes) and subsequently immersed in aqueous copper perchlorate solutions with different concentrations. A paper-strip immersed in water was also measured. Photos were recorded using an iPhone 8. Emission spectra of paper strips were acquired in the same spectrofluorometer, using an appropriate accessory for solid samples.

Results and discussion

Synthesis

Chalcones present several structural features, particularly in terms of synthetic flexibility, which allows for functionalization of its core through simple procedures, with relatively moderate to high reaction yields. The synthesis of the two chalcone-DPA chemosensors is described in Figure 2.

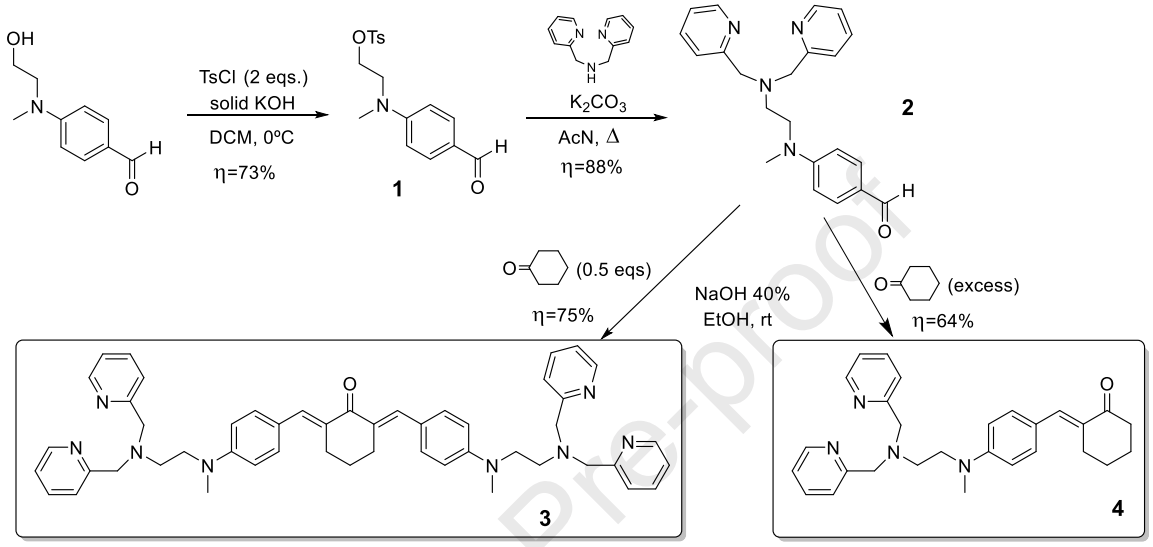

Figure 2. Synthetic scheme for chalcones **3** and **4**.

Briefly, the hydroxy group of *N*-methyl-*N*-(2-hydroxyethyl)-4-aminobenzaldehyde was tosylated, followed by an S_N2 reaction with di-(2-picolyl)amine, to afford **2**. Finally, condensation under basic conditions with either one equivalent or excess of cyclohexanone resulted in chemosensors **3** and **4**, respectively. Structural characterization of both chemosensors was performed by HRMS and NMR spectroscopy. For chemosensor **4**, single crystals were obtained readily from the purified fraction of the column, upon solvent removal (see figure 3, and Supplementary Material for X-Ray crystallography data). A detailed analysis of 1D and 2D NMR spectra, as well as the respective mass spectra, has allowed for a full structural characterization of all products (see Supplementary Material, figures S1-S24 and tables S1-S4).

UV-Vis and fluorescence studies

As mentioned above, the substitution pattern of the chalcone core has significant influence in its optical properties, according to the electronic nature (withdrawing or donating) of the substituent group, and to its relative position. In this particular case, an amino group in position 4 exerts a strong "push-pull" effect, since it is directly in resonance with the carbonyl group from the chalcone. We performed UV-Vis and fluorescence spectra of **3** in solvents with different polarities, and found that there is a linear relationship between the Stokes' shift and the ET(30) value of the solvent (figure S25).

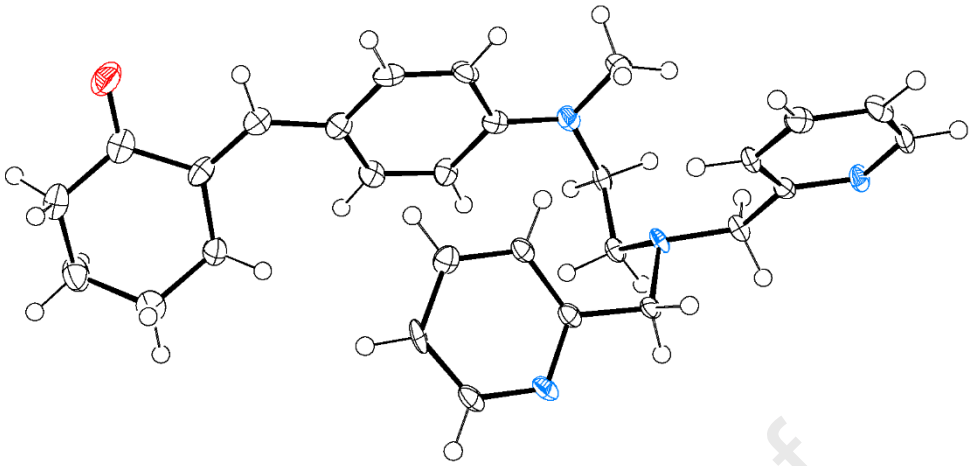

Figure 3. ORTEP-3 diagram of compound **4** (asymmetric unit), using 50% probability level ellipsoids.

This result confirms the strong intramolecular charge-transfer (ICT) character of chemical structure of **3**, typical for planar (or *quasi* planar) aromatic amines [26]. The values for molar extinction coefficient at the absorption maxima and fluorescence quantum yields for both chemosensor **3** and **4** can be found in table 1.

Table 1. UV-Vis and luminescent spectral data for chemosensors **3** and **4**, in MeOH/HEPES 10 mM pH 7 (1:1).

	λ_{max} (nm)	$\lambda_{emission}$ (nm)	Stoke's shift (cm^{-1})	ε^{*} (M^{-1} cm^{-1})	Φ^{**}
3	470	610	4883	38531	0.016
4	398	498	5045	24645	0.0006

*Molar extinction coefficient at λ_{max}; **Fluorescence quantum yield

The ability of chalcones **3** and **4** to act as sensors for metal ions in aqueous media requires that the DPA units are deprotonated at neutral pH. Taking this into account, a pH titration was performed and followed simultaneously by UV-Vis and fluorescence spectroscopy. The spectra indicate that pH has very little influence on the optical properties of both **3** and **4** in the pH range from 3 to 10 (figure S26). Indeed, the protonation of the aliphatic nitrogen from the DPA units, which occurs at ca. pH~5 (pK_{a1}[**3**] = 4.7; pK_{a1}[**4**] = 5.0) [27], has very little effect on the luminescent properties of **3** or **4**, suggesting minor influence of photoinduced electron transfer effects, as opposed to previously reported fluorescent DPA systems.[7,27] Only at very acidic conditions can one observe the protonation of the lone pairs of electrons from the nitrogens that are directly conjugated with the chalcones, due to the electron-withdrawing effect from the carbonyl group (fig. S27), with pKa values below 1 (pK_{a2}[**3**] = pK_{a2}[**4**] = 0.75). A summary for the pH dependent equilibria is described in scheme S1.

In order to assess the sensitivity and selectivity of chemosensors **3** and **4** in molecular recognition of cations, a simple test was performed by adding two equivalents of different divalent cations. The results show that Cu^{2+} is the cation that induces the strongest effect, both in the UV-Vis and fluorescence spectra (figures 4 and S28). Indeed, a full titration of both **3** and **4** with Cu^{2+} cations results in a colorimetric response, with sensor **3** changing its color from orange to pale yellow, while chemosensor **4** changes from pale yellow to colorless (figures 4A and 4B). This naked-eye observation is consistent with the observed hypsochromic shift in UV-Vis absorption maxima for both chemosensors in the presence of Cu^{2+}, a behavior similar to the protonation of **3** and **4** at pH values below 1 (figures 4C and 4E).

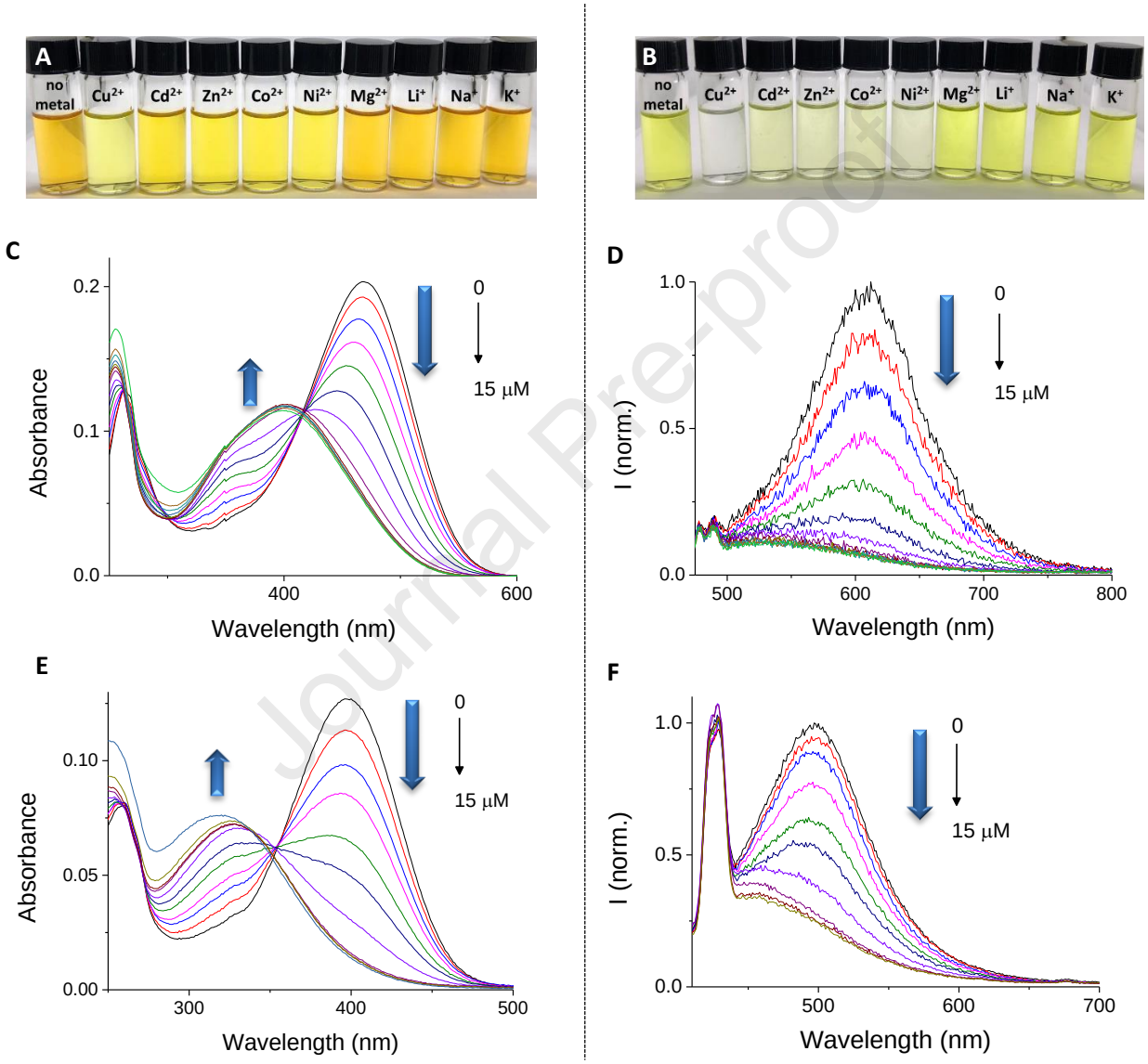

Figure 4. Naked-eye sensitivity of chemosensors **3** (A) and **4** (B) (5 μM) towards different metal ions (top); UV-Vis and emission spectra of chemosensors **3** (C and D) and **4** (E and F), with increasing amounts of Cu^{2+}, in MeOH/HEPES 10 mM pH 7 (1:1). λ_{exc} (**3**) = 419 nm; λ_{exc} (**4**) = 375 nm.

This result seems to indicate that the nitrogen which is directly conjugated with the chalcone core is also participating in the coordination process of Cu^{2+}, being this effect much stronger for this

metal when compared to all the other studied metal cations. The emission spectra of both chemosensors reveal a strong fluorescence quenching in the presence of Cu^{2+} cations (figures 4D and 4F), reaching a plateau after the addition of roughly 1 equivalent of metal (see figures 6C and 6D, below), for both chemosensors. Method for continuous variation yielded the respective Jobs' plot, which indicated a 1:1 stoichiometry between each chemosensor and Cu^{2+} (figure 5). Additional MALDI-TOF-MS experiments also confirmed the presence of the 1:1 binding products for both chemosensors with Cu^{2+} (figures S29 and S30).

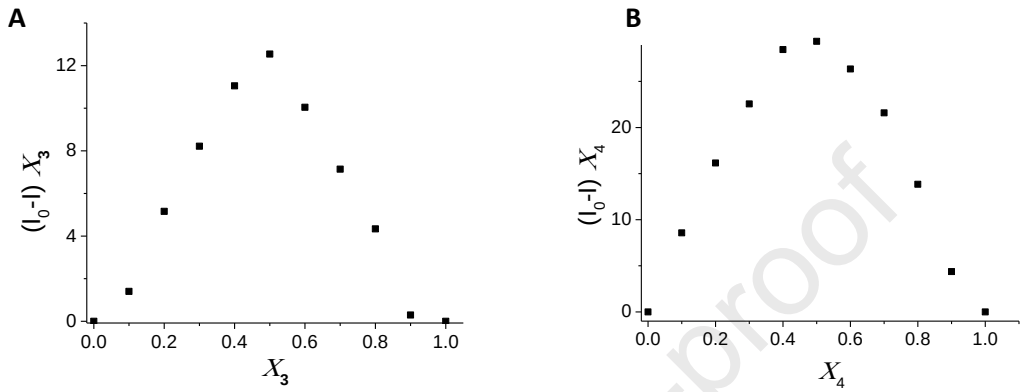

Figure 5. Job's plot for **3** (A) and **4** (B) in the presence of Cu^{2+}. For both cases, the intercept of the slope of the curves is at $X_{sensor} \sim 0.5$. Conditions: 1:1 MeOH/10mM HEPES pH7, λ_{exc} (**3**) = 470 nm; λ_{exc} (**4**) = 342 nm.

While this behavior is expected for chemosensor **4**, these results suggest that, although chemosensor **3** possesses two DPA centers, binding the first Cu^{2+} cation renders the second DPA chelating moiety "inactive". An explanation can be that the "free" electron pair from the nitrogen which is conjugated to the chalcone opposite to the first Cu^{2+}-DPA coordination sphere is now less available for coordinating a second metal cation, due to a change in the global polarity/charge density of the chromophore core (see scheme 1). The limit of detection [19] for each of the chemosensors towards Cu^{2+} was found to be 0.379 µM and 0.442 µM for chemosensors **3** and **4**, respectively.

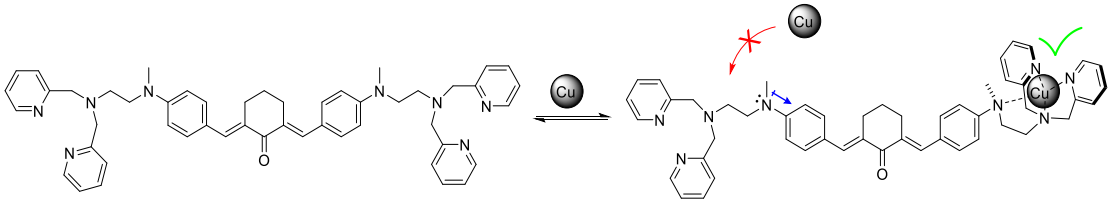

Scheme 1. Proposed binding mechanism of Cu^{2+} to chemosensor **3**. Upon binding to one DPA center, the nitrogen lone-electron pair from the second DPA is no longer available for coordinating a second Cu^{2+} cation.

Metal selectivity

Although both chemosensors have a significantly higher affinity towards Cu^{2+} ions, the results from figure S27 indicate some competitivity for binding for several metal ions, namely Cd^{2+}, Zn^{2+}, Co^{2+} and Ni^{2+}. This is also reflected in the naked-eye experiments in figure 3. As such, full titration of these metal competitors was also performed by following UV-Vis and emission changes in the presence of each of these ions (figure 6). For Cd^{2+} and Zn^{2+}, although UV-Vis spectra indicate some metal binding takes place, negligible changes are observed in the emission properties of both chemosensors. Co^{2+} and Ni^{2+} induce a similar behavior as Cu^{2+} for both chemosensors, although the spectral changes occur to a lesser extent, particularly if we compare UV-Vis spectra. These results, along with those for Cu^{2+} (for comparison purposes), are summarized in figure 6.

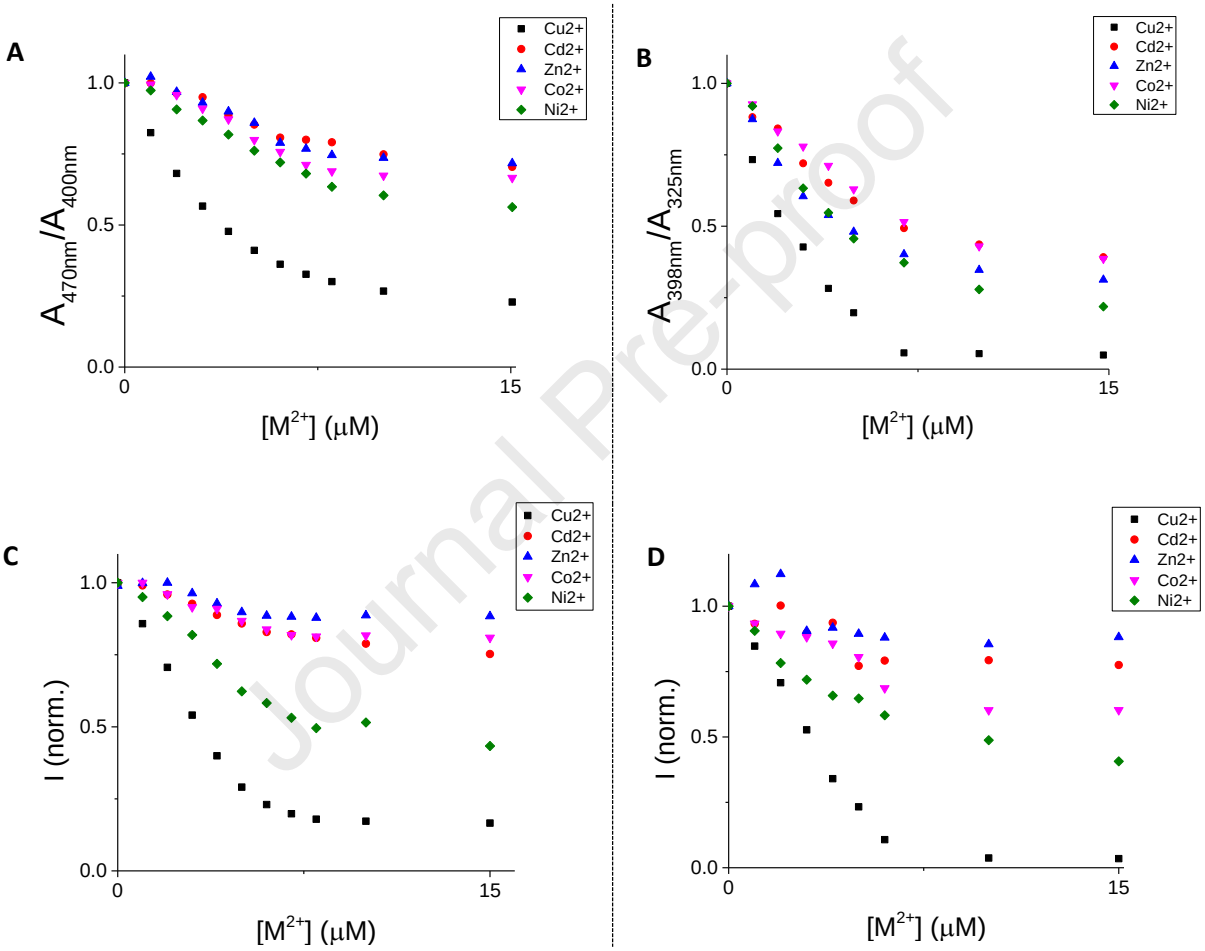

Figure 6. Changes in the optical properties of **3** and **4** (5 μM) in the presence of different metal ions. (a) and (b): ratio between UV-Vis maxima of free and metal-bound chemosensors **3** and **4**, respectively; (c) and (d): luminescence of **3** and **4** in the presence of increasing amounts of metal ions, respectively [λ_{exc} (**3**) = 419 nm; λ_{exc} (**4**) = 375 nm].

The luminescent emission data sets were fitted to a 1:1 binding model, yielding the corresponding association constants for each of the studied metals (table 2). The highest constant was determined for Cu^{2+}, which indicates some selectivity from chemosensors **3** and **4** towards this cation. Other studied metals also present high association constants, being Co^{2+} and Ni^{2+} the strongest

interferents, with K_a only 5 to 10 times lower than that of Cu^{2+} for **3** and **4**. However, it is noteworthy that Cu^{2+} is the cation that induces the strongest quenching effect on the luminescence of both **3** and **4** (table 2). The observed values for both association constants and limits of detection is comparable to other reported optical sensor systems for Cu^{2+}.[28]

Table 2. Association constants (K_a) and signal variation (Δ[%]) for chemosensors **3** and **4** with metal ions.

	3		**4**	
Metal ion	K_a (M^{-1})	Δ[%]	K_a (M^{-1})	Δ[%]
Cu^{2+}	6.2×10^6	84	4.1×10^6	96
Cd^{2+}	4.9×10^5	24	n.d.	23
Zn^{2+}	1.0×10^6	14	n.d.	12
Co^{2+}	1.6×10^6	19	1.4×10^5	40
Ni^{2+}	7.0×10^5	59	4.4×10^5	59

Competitive studies were also conducted, where each of the metals (2 equivalents) is added to a chemosensor solution prior to Cu^{2+} addition (2 equivalents), thus allowing to assess their degree of competition for binding to chalcones **3** and **4**. The results are shown in figure 7.

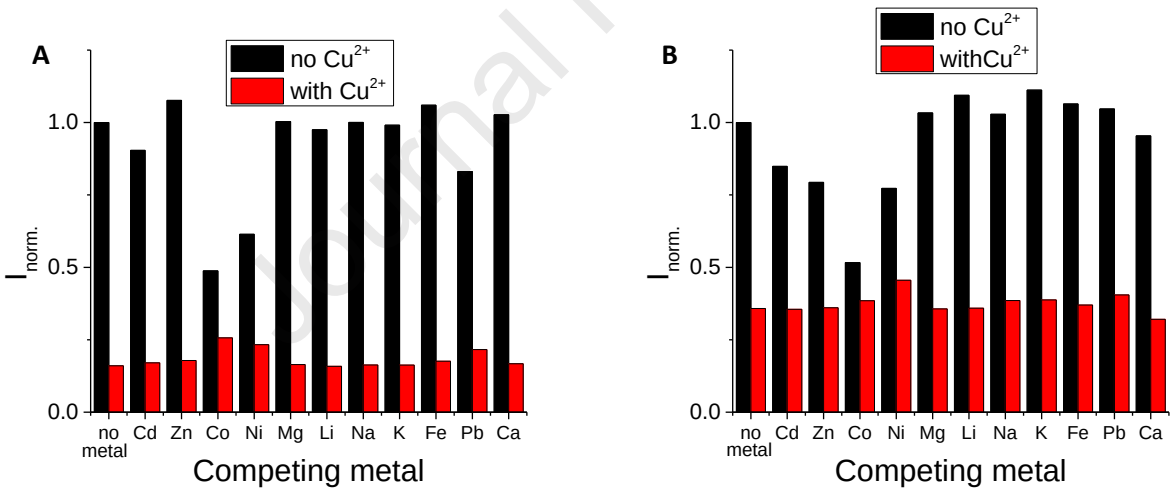

Figure 7. Competitive binding of chemosensors **3** (A) and **4** (B) to Cu^{2+}, in the presence of other metal ions.

Once again, for both chemosensors, the strongest competitors for Cu^{2+} binding are Ni^{2+} and Co^{2+} but a clear preference for Cu^{2+} is observed in all cases, demonstrating some degree of specificity of these host molecules for this cation. Nevertheless, it should be stressed out that, for Ni^{2+} (or Co^{2+}) rich environments, prior sample treatment with appropriate selective chelators is needed in order to determine Cu^{2+} content using our chemosensors.

Paper test-strips

For further assessing the application of these chemosensors as a rapid method for detecting copper levels in water samples, paper test-strips were prepared with chemosensor **3** by impregnation in a concentrated methanolic solution ([**3**] ~ 0.3 mM). This chemosensor was chosen since it presents a better naked-eye color contrast than chemosensor **4**. The paper strips were left to dry for 15 minutes on air and were afterwards immersed into aqueous solutions of different copper concentrations and once more left to dry (figure 8A). Upon drying, the luminescence of the paper strips under 365 nm UV light (figure 8B) and the corresponding spectra were recorded (figure 8C).

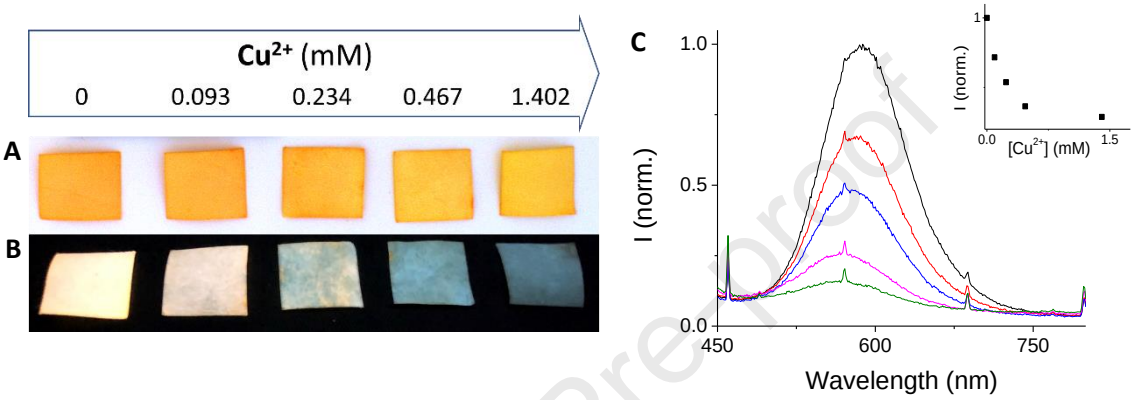

Figure 8. Photos of paper-strips (A) on ambient light and (B) under UV light (365 nm), and (C) respective emission spectra [λ_{exc} (**3**) = 419 nm], upon exposure to different Cu^{2+} concentrations.

Under ambient light, the test-strips reveal a slight change in color, from orange to yellow (fig. 8A), in line with what was recorded in solution. Moreover, the detection of copper exposure is much clearer under a UV lamp, where the strong luminescence in the absence of metal is almost fully quenched in the presence of Cu^{2+} (fig. 8B), which is further highlighted in the recorded emission spectra (fig. 8C). The inset from fig. 7C indicates a high sensitivity in concentrations up to *ca.* 0.5 mM of Cu^{2+}. These results show that the developed paper strips can detect Cu^{2+} in the high micromolar/low millimolar range, which can be useful for a rapid screening on monitoring copper levels in mining waste waters and nearby water sources, typically found in these concentrations.[29,30]

Conclusions

The new DPA-chalcone sensors are capable of selectively detect Cu^{2+} in solution through naked-eye color changes and luminescence quenching, even in the presence of other metal cations. Both chemosensors binding copper ions through a 1:1 stoichiometry, with association constants and limits of detection comparable to other reported systems. Paper test-strips prepared with one chemosensor allowed for the detection of Cu^{2+} in the high-micromolar/low-millimolar concentration range, highlighting the applicability of these systems for monitoring this metal in mining wastewater samples.

Acknowledgements

This work was supported by the Associate Laboratory for Green Chemistry - LAQV which is financed by national funds from FCT/MCTES (UIDB/50006/2020 and UIDP/50006/2020). The NMR spectrometers are part of Rede Nacional de RMN (PTNMR), supported by FCT/MCTES (ROTEIRO/0031/2013 - PINFRA/22161/2016) (co-financed by FEDER through COMPETE 2020, POCI, and PORL and FCT through PIDDAC). T.M. acknowledges PhD grant SFRH/BD/139171/2018 from FCT/MCTES, for the financial support. L. J. G. acknowledges FCT/MCTES for financial support from "Escola de Verão LAQV-NOVA - Iniciação à Investigação em Química Verde", under the program "Verão com Ciência". The Spanish Ministerio de Ciencia e Innovación (Project PID2019-104121GB-I00) is also aknowledged.

References

[1] Wu D, Sedgwick AC, Gunnlaugsson T, Akkaya EU, Yoon J, James TD. Fluorescent chemosensors: The past, present and future. Chem Soc Rev 2017;46:7105–23.

[2] Jeong Y, Yoon J. Recent progress on fluorescent chemosensors for metal ions. Inorganica Chim Acta 2012;381:2–14.

[3] Liu Z, He W, Guo Z. Metal coordination in photoluminescent sensing. Chem Soc Rev 2013;42:1568–600.

[4] Gale PA, Howe ENW, Wu X. Anion Receptor Chemistry. Chem 2016;1:351–422.

[5] Niklas N, Wolf S, Liehr G, Anson CE, Powell AK, Alsfasser R. Ni(II), Cu(II) and Zn(II) complexes of a bifunctional bis(picolyl)amine (bpa) ligand derived from glycine. Inorganica Chim Acta 2001;314:126–32.

[6] Palaniandavar M, Butcher RJ, Addison AW. Dipicolylamine Complexes of Copper(II): Two Different Coordination Geometries in the Same Unit Cell of Cu(Dipica)2(BF4)2. Inorg Chem 1996;35:467–71.

[7] Jiang W, Fu Q, Fan H, Wang W. An NBD fluorophore-based sensitive and selective fluorescent probe for zinc ion. Chem Commun 2008:259–61.

[8] Xu Z, Kim GH, Han SJ, Jou MJ, Lee C, Shin I, et al. An NBD-based colorimetric and fluorescent chemosensor for Zn2+ and its use for detection of intracellular zinc ions. Tetrahedron 2009;65:2307–12.

[9] Zhang Y, Guo X, Zheng M, Yang R, Yang H, Jia L, et al. A 4,5-quinolimide-based fluorescent sensor for the turn-on detection of Cd2+ with live-cell imaging. Org Biomol Chem 2017;15:2211–6.

[10] Xiong JK, Wang KR, Wang KX, Han TL, Zhu HY, Rong RX, et al. Fluorescent enhancement sensing of cadmium (II) ion based on a perylene bisimide derivative. Sensors Actuators, B Chem 2019;297:126802.

[11] Hu Y, Ke Q, Yan C, Xu CH, Huang XH, Hu SL. A new fluorescence chemosensor for selective detection of copper ion in aqueous solution. Tetrahedron Lett 2016;57:2239–43.

[12] Moro AJ, Santos M, Outis M, Mateus P, Pereira PM. Selective Coordination of Cu2+ and Subsequent Anion Detection Based on a Naphthalimide-Triazine(DPA)2 Chemosensor. Biosensors 2020;10:1–11.

[13] Gupta A, Garg S, Singh H. Development of chalcone-based derivatives for sensing applications. Anal Methods 2020;12:5022–45.

[14] Ballesteros JF, Sanz MJ, Ubeda A, Miranda MA, Iborra S, Payá M, et al. Synthesis and Pharmacological Evaluation of 2′-Hydroxychalcones and Flavones as Inhibitors of Inflammatory Mediators Generation. J Med Chem 1995;38:2794–7.

[15] Ahmad W, Kumolosasi E, Jantan I, Bukhari SNA, Jasamai M. Effects of novel diarylpentanoid analogues of curcumin on secretory phospholipase A2, cyclooxygenases, lipo-oxygenase, and microsomal prostaglandin e synthase-1. Chem Biol Drug Des 2014;83:670–81.

[16] Won SJ, Liu CT, Tsao LT, Weng JR, Ko HH, Wang JP, et al. Synthetic chalcones as potential anti-inflammatory and cancer chemopreventive agents. Eur J Med Chem 2005;40:103–12.

[17] Anto RJ, Sukumaran K, Kuttan G, Rao MNA, Subbaraju V, Kuttan R. Anticancer and antioxidant activity of synthetic chalcones and related compounds. Cancer Lett 1995;97:33–7.

[18] Ishitsuka H, Ninomiya YT, Ohsawa C, Fujiu M, Suhara Y. Direct and specific inactivation of rhinovirus by chalcone Ro 09-0410. Antimicrob Agents Chemother 1982;22:617–21. https://doi.org/10.1128/AAC.22.4.617.

[19] Chen M, Zhai L, Christensen SB, Theander TG, Kharazmi A. Inhibition of fumarate reductase in Leishmania major and l. donovani by chalcones. Antimicrob Agents Chemother 2001;45:2023–9.

[20] Domínguez JN, León C, Rodrigues J, De Domínguez NG, Gut J, Rosenthal PJ. Synthesis and antimalarial activity of sulfonamide chalcone derivatives. Farmaco 2005;60:307–11.

[21] Vatsadze SZ, Gromov SP. Novel linear bis-crown receptors with cross-conjugated and conjugated central cores. Macroheterocycles 2017;10:432–45.

[22] McNaught AD, Wilkinson A. International Union of Pure Appl. Chem. Compendium of Chemical Terminology (' "The Gold Book"') 1997.

[23] Olmsted J. Calorimetric determinations of absolute fluorescence quantum yields. J Phys Chem 1979;83:2581–4.

[24] Reynolds GA, Drexhage KH. New coumarin dyes with rigidized structure for flashlamp-pumped dye lasers. Opt Commun 1975;13:222–5.

[25] Thordarson P. Determining association constants from titration experiments in supramolecular chemistry. Chem Soc Rev 2011;40:1305–23.

[26] Valeur B. Molecular Fluorescence: Principles and Applications. vol. 8. 2001, 62–67.

[27] Moro AJ, Cywinski PJ, Körsten S, Mohr GJ. An ATP fluorescent chemosensor based on a Zn(ii)-complexed dipicolylamine receptor coupled with a naphthalimide chromophore. Chem Commun 2010;46:1085–7.

[28] Sivaraman G, Iniya M, Anand T, Kotla NG, Sunnapu O, Singaravadivel S, et al. Chemically diverse small molecule fluorescent chemosensors for copper ion. Coord Chem Rev 2018;357:50–104.

[29] Santoro S, Estay H, Avci AH, Pugliese L, Ruby-Figueroa R, Garcia A, et al. Membrane technology for a sustainable copper mining industry: The Chilean paradigm. Clean Eng Technol 2021;2:100091.

[30] Hadži Jordanov S, Maletić M, Dimitrov A, Slavkov D, Paunović P. Waste waters from copper ores mining/flotation in'Bučbim' mine: characterization and remediation.

Highlights

- Two new chalcone-based fluorescent chemosensors, possessing one or two di-(2-picolyl)amine units, are presented
- Both sensors present a strong intramolecular charge transfer (ICT) character, exhibiting a large Stoke's shift
- A higher sensitivity is observed towards copper (II), with strong UV-Vis and fluorescent responses
- Paper test-strips were prepared with one of the chemosensors as a rapid monitoring method for Cu (II) in water samples

NOVA SCHOOL OF
SCIENCE & TECHNOLOGY

DEPARTAMENTO
DE QUÍMICA

DEPARTMENT
OF CHEMISTRY

Conflict of Interest

The authors of the manuscript entitled *"Chalcone-based fluorescent chemosensors as new tools for detecting Cu^{2+} ions"*, declare no conflict of interest, upon submission to the journal *Dyes and Pigments*.

Campus de Caparica
2829-516 Caparica | Portugal
T. +351 212 948 575
dq.secretariado@fct.unl.pt
www.fct.unl.pt